Journal of Solid Mechanics and Materials Engineering

Vol.3, No.11, 2009

Finite Element Analysis and Experiment of the Subsurface Damages on Silicon Nitride Subjected to Repeated Impact Loadings*

Fergyanto E. GUNAWAN**, Hiroomi HOMMA*** and Satryo S. BRODJONEGORO†

** Institute of Solid Mechanics, Braunschweig University of Technology
D-38016, Braunschweig, Germany
E-mail: f.e.gunawan@gmail.com and f.gunawan@tu-bs.de

*** International Cooperation Center for Engineering Education Development
1-1 Hibarigaoka, Tempaku-cho, Toyohashi-shi, 441-8580, Japan

† Department of Mechanical Engineering, Toyohashi University of Technology
1-1 Hibarigaoka, Tempaku-cho, Toyohashi-shi, 441-8580, Japan

Abstract

This paper presents characterization and evaluation of a silicon nitride plate subjected to repeated impact by a small but hard particle at velocity in a range from 80 to 160 m/s. It specifically focuses on damage patterns in relation to repeated impacts. In addition, the paper also provides a finite element analysis in conjunction with the Tuler-Butcher damage model that is employed to study the formation of the damages during the multiple impact events. The results of the analysis using a very fine mesh indicated that during the contact of the projectile and the plate, the area beneath the contact surface is mainly governed by a compressive stress state. However, a small-adjacent area encircled the compressed region was in a high tensile stress state. The largest tensile stress in the area instantly occurred after the projectile touched the ceramic within a time significantly shorter than the time required for the maximum contact. Majority of the ring cracks observed in the experiments occurred in this area. Furthermore, the ring cracks grew upon further application of impact. Finally, the analysis indicated that the growth of the ring crack led to formation of the spall or the cone crack.

Key words : Ceramics, Brittle Fracture, Damage Mechanics, Fracture Mechanics, Impact Strength

1. Introduction

Ceramic materials have been widely used as a protective material in many engineering applications. For examples: in the hybrid armor system, the ceramic that sandwiched with a composite plate is used to destroy the tip of a coming projectile, to distribute the load delivered by the projectile to a large area such that the load can be efficiently be sustained by the composite, and to stop the projectile[1],[2]. In a system of the gas turbine, the ceramic is used to protect the turbine blade from being exposed to high temperature and to improve the wearability against impact with high speed particles[3]. In those systems, ceramic material becomes a material of choice because their high compressive strength and low density[4].

Because of their importance, a number of studies has been addressed to the response of the ceramic materials subjected to quasi-static and high strain rate loading conditions. Those studies concluded that the ceramic materials behaves elastic when the confining pressure is low, but they behaves ductile when the confining pressure is high. The material is also ductile as marked with existing significant plastic flow when it is subjected to an extremely high loading rate[5]. If the magnitude of the compressive wave exceeds the material Hugoniot elastic limit (HEL), damage begins to accumulate through formation of cracks; however, the

*Received 11 May, 2009 (No. 09-0195)
[DOI: 10.1299/jmmp.3.1160]

material strength increases as the pressure increasing even beyond the HEL. Accumulation of the cracks may lead to the spalling and also may form a major crack that propagates within the material at a speed of the elastic wave velocity and lead to major conoid fragments or splitting of the tested specimen into some major pieces[(2), (4), (6), (7)].

However, the existing publications seems to overlook a fact that the ceramic material, for an example in a protecting a turbine blade, is often damaged by repeated impact of small but hard particles. Therefore, this study brings attention into such a problem, and specifically, focuses on the formation and evolution of damages in a ceramic material when the material is repeatedly impacted.

2. Experimental Setup and Results

2.1. Experimental Apparatus

A gas gun system as schematically shown in Fig. 1 was used in introducing damages to the ceramic material. The main components of the system consist of the projectile, the reservoir, the hollow cylindrical barrel, and the velocity measurement system. The projectile was placed at the end of the barrel, and helium gas that compressed in the reservoir was released at a controlled pressure to accelerate the projectile in the barrel to the other end where the specimen was placed nearby. The gas gun system allows us to easily produce the repeated impact loading at a controlled velocity.

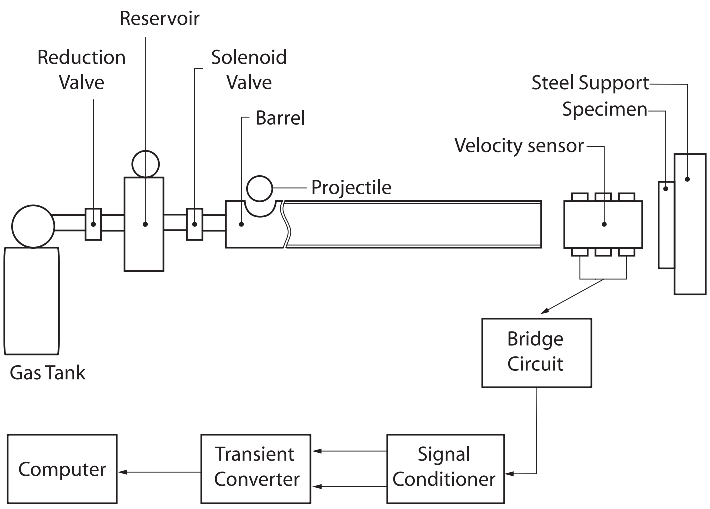

Fig. 1 Experimental setup

The specimen was a silicon nitride, Si_3N_4, block having dimension of $30 \times 30 \times 5$ mm. This particular material has relatively good shock resistance in comparison to other ceramics. Table 1 shows the physical and mechanical properties of the specimen.

Table 1 The physical and mechanical properties of the specimen.

Properties	Value	Unit
Density	3,200	kg/m^3
Porosity	0.1	%
Bending strength	880.0	MPa
Fracture toughness	6.0	MPa $\sqrt{m}$
Young's modulus	290.0	GPa
Poisson's ratio	0.28	
Hardness	92	HRA

The specimen was placed on a 15 mm thick steel plate, and its circumferential was constrained by a rubber.

The repeated impact loading was generated by impacting 2 mm diameter sphere projectiles made of stainless steel SUS304 material having a density of $8,000$ kg/m^3, a mass of 30×10^{-3} kg, Young's modulus of 200 GPa, and Poisson's ratio of 0.3. At a fixed projectile velocity, the specimen was repeatedly impacted, and the damage on its impacted surface was observed. After certain number of impacts, the damage within the ceramic was also observed by using the scanning electron microscope (SEM). The pressure in the reservoir was controlled such that the projectile reached the ceramic at velocities of 80, 100, 120, 140, and 160 m/s.

2.2. Experimental Results

Prior the experiment, the specimens front surface, where the impact would be applied, and the their cross-section surface were observed using SEM for the existing flaws. Delagrave[(8)], cited by Ref. (9), suggests that the flaw distribution in a ceramic can alter its ballistic performance considerably. Since the ballistic performance is directly related to the damage formation; therefore, the flaw distribution affects the damage formation. The observation found that the largest diameter of the flaw on the specimen front surface is 4 μm. Figures 2 and 3 shows the SEM figures of the specimen front and cross-section surfaces.

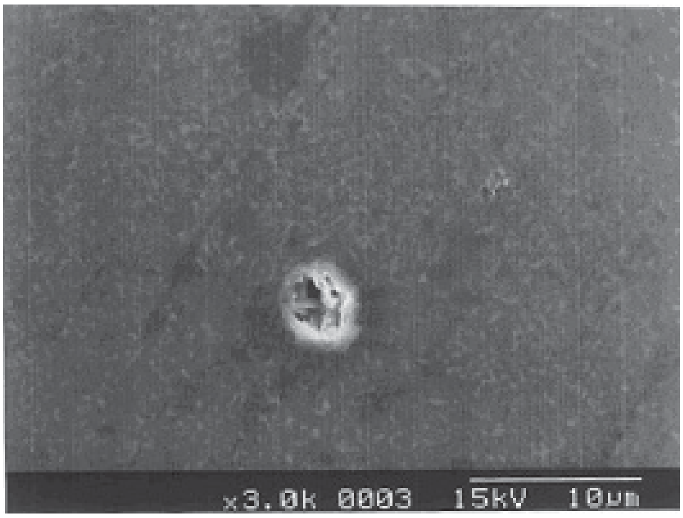

Fig. 2 The front surface of the non impacted specimen.

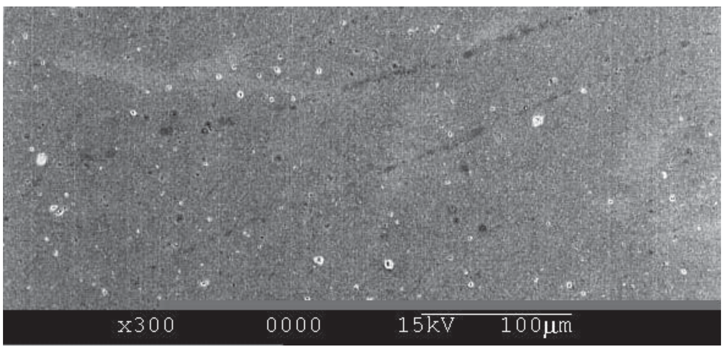

Fig. 3 The cross-section surface of the non impacted specimen.

After the observation of the existing flaws, the specimens were installed to the gas gun system; then, they were repeatedly impacted with a sphere steel ball; and then, the front surfaces were observed for every 20 impacts.

For the impact velocities of 80–120 m/s, a number of figures, two of them are reproduced in Figs. 4 and 5, obtained by SEM show that the specimens were intact without any significant

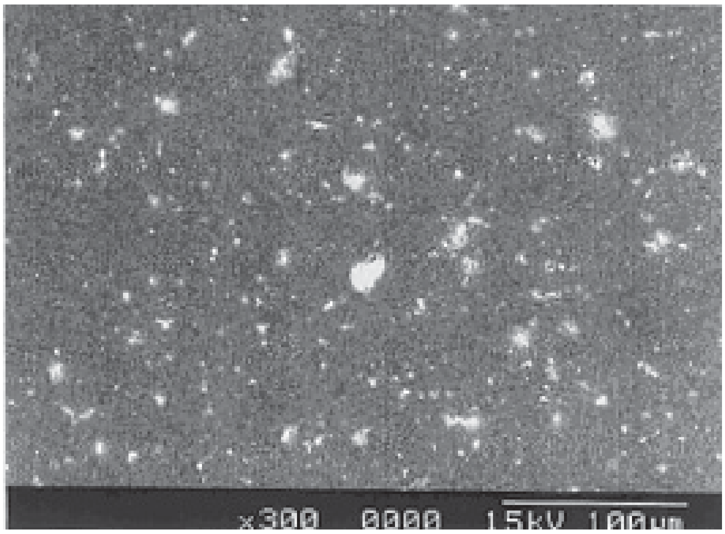

Fig. 4 Surface of the specimen after 3600 impacts at velocity 80 m/s.

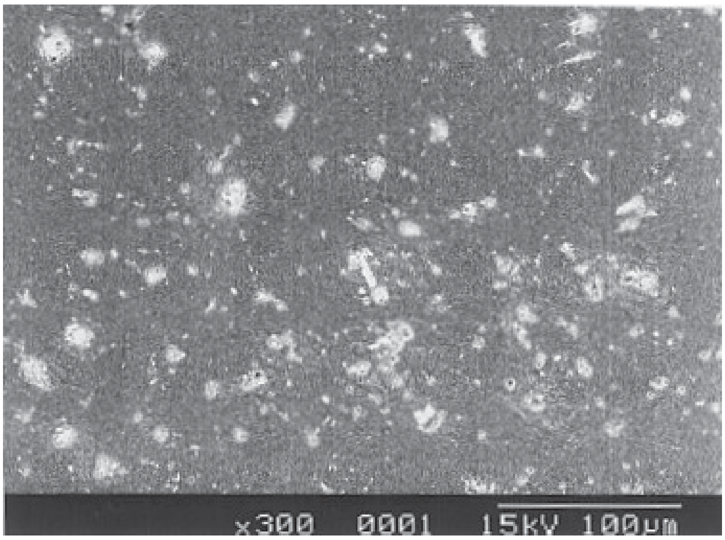

Fig. 5 Surface of the specimen after 3600 impacts at velocity 120 m/s.

damages even after 3600 impacts. However, the largest diameter of the flaws on the surface of those specimens grew to 19, 23, and 26 μm for impact velocities of 80, 100, and 120 m/s, respectively.

For the impact velocity of 140 m/s, concentric cracks occurred on the front surface. Those cracks are clearly shown in Fig. 6 and 7. In Fig. 6, a major concentric crack seems connecting the surface defects or flaws on the specimen front surface. Figure 7 shows that those concentric cracks are localized within an annulus with an inner radius of 0.08 mm and an outer radius of 0.16 mm; significantly smaller than the impactor radius of 1 mm. At this impact velocity, the annulus was severely damaged after 480 impact. Figure 8 shows two large spalls on the annulus have been removed.

The cone cracks with an angle of about 45 degrees and a maximum length about 200 μm were observed in a specimen subjected to 500 impacts at 140 m/s velocity. The cone cracks are shown in Fig. 11.

For the impact velocity of 160 m/s, 60 impacts have produced significant number of concentric cracks, and at 220 impacts, a large spall was removed from the specimen front

Vol.3, No.11, 2009

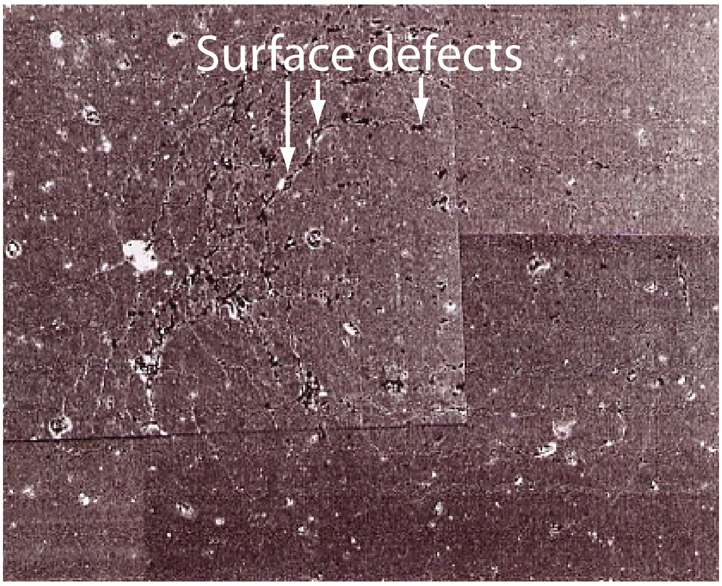

Fig. 6 Surface of the specimen after 400 impacts at velocity 140 m/s.

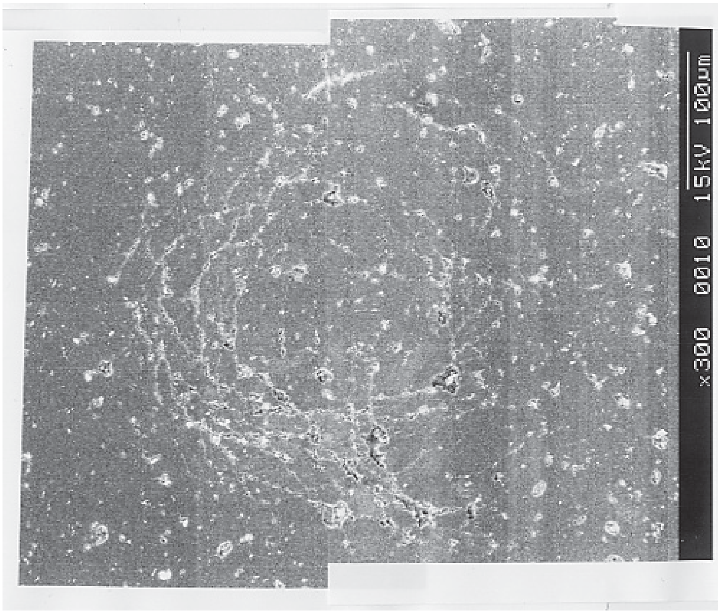

Fig. 7 Surface of the specimen after 560 impacts at velocity 140 m/s.

surface.

3. Numerical Analysis

The experimental results, presented in Sec. 2.2, has shown that the failure on this particular ceramic in the present loading conditions started from the formation of tiny cracks. Those tiny cracks localized and gradually grew. Upon further application of the impact loads, those tiny cracks formed spalls, and some cracks led to formation of the cone cracks. This damage development is similar to those occurred in quasi-brittle materials such as concrete where the failure started from the formation of cracks, and the propagation of the newly formed cracks or the existing defects as observed in Ref. (10). To study development and formation of those damages, a number of finite element analysis was performed by means a commercial finite element package LS-DYNA v. 971. In this section, the detail finite element analysis is described, and the analysis results are provided.

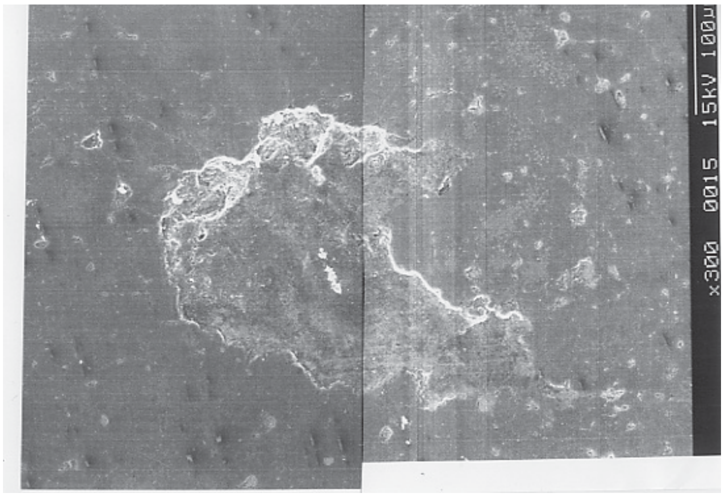

Fig. 8 Surface of the specimen after 1060 impact at velocity of 140 m/s.

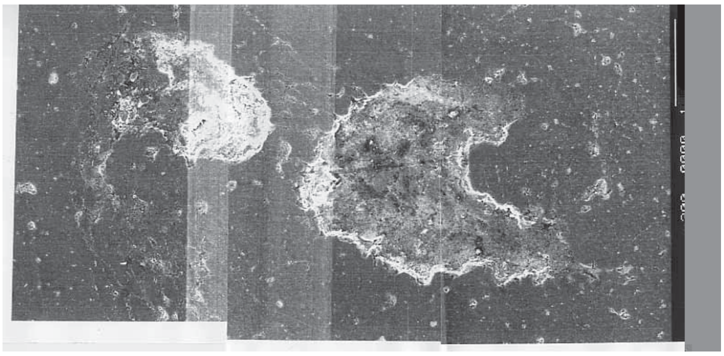

Fig. 9 Surface of the specimen after 1120 impact at velocity of 140 m/s.

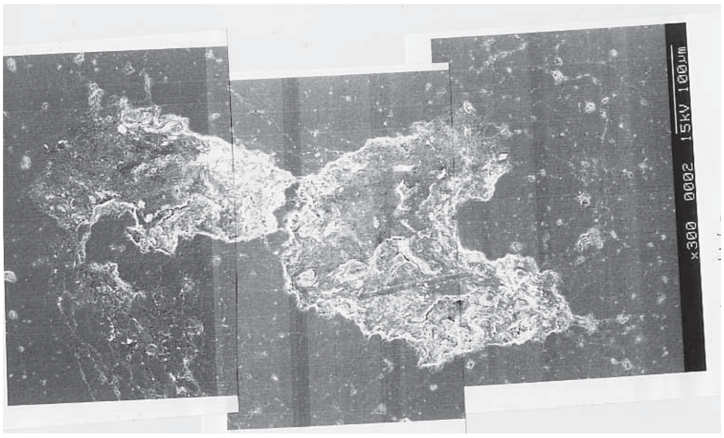

Fig. 10 Surface of the specimen after 1160 impact at velocity of 140 m/s.

3.1. The Finite Element Model Mesh

The finite element mesh model of the sphere impactor and the ceramic plate are depicted in Fig. 12. The model consists of 12625 nodes and 22730 linear-axisymmetric elements. Those nodes on the bottom of the ceramic plate were constrained in movement in the thickness direction. This is due to the fact that in the experiments, the ceramic plate was firmly pressed against a thick steel plate. Furthermore, the experiments have shown that the damages occurred in a small area within a radius of 0.2 mm, and a depth of 0.2 mm. Hence, in the model, a very fine mesh was employed to an area of size 0.5×0.5 mm^2 or more than twice

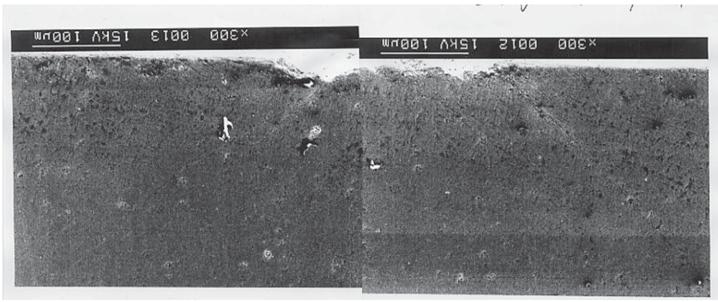

Fig. 11 Surface of the specimen cross-section after 500 impacts at velocity of 140 m/s.

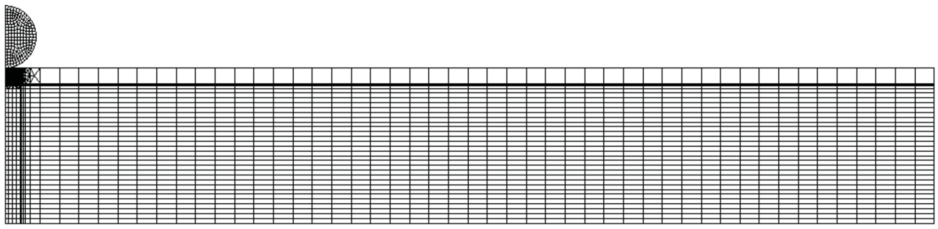

Fig. 12 The axisymmetric finite element model of the sphere and the specimen.

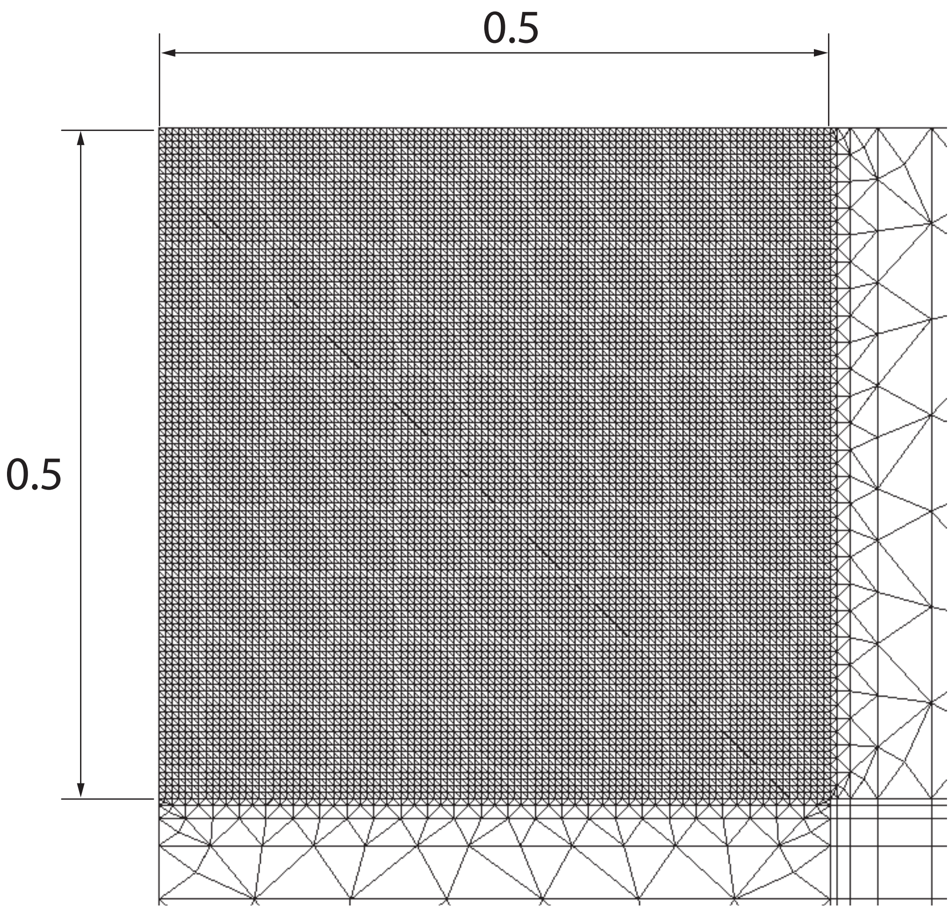

Fig. 13 The finite element model mesh of the damaged area. Unit is mm

larger than the damaged area as show in Fig. 13. The area was meshed using the triangle elements with an side length of 5×10^{-3} mm. Such a mesh allows a crack to propagate almost isotropically[(11)]. Therefore, the above model is reasonably accurate to capture the damage formation in the macroscopic scale.

The interaction between the sphere and the plate is crucial in this study because the observed damages occurred and concentrated in this area. It is extremely important to simulate the interaction accurately. Therefore, the penalty method that allows us to manually adjust the penalty stiffness, a non-dimensional parameter, is employed to prevent the sphere penetrating the ceramic surface. In LS-DYNA version 971, the method has been implemented in the *CONTACT_2D_AUTOMATIC_SINGLE_SURFACE card. In implementing the method, the stiffness was carefully adjusted such that the interaction is smooth, and the sphere and ceramic surfaces closely interact to each other during impact. As results, for the optimum contact stiffness of $1.0 \times 10^{+20}$, the sphere can be fully restrained from penetrating the ceramic surface as shown in Fig. 14. The right panel in the figure shows that during the impact, the

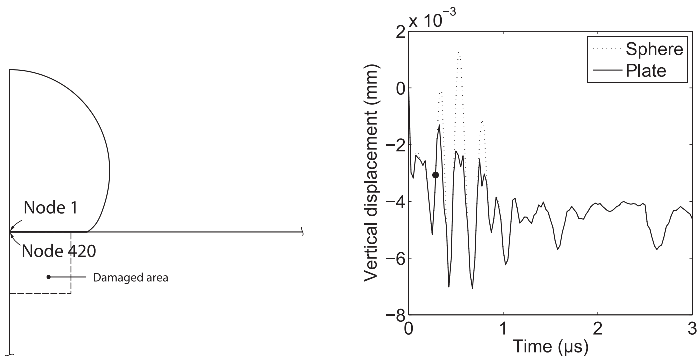

Fig. 14 Left panel: the maximum contact area between the sphere and the plate occurred at 6.4 μs. Right panel: vertical displacements of Node 1 on the sphere and Node 420 on the plate. The damage is firstly initiated at a time marked by •.

both sphere and plate interact closely although highly fluctuating. Furthermore, a comparison to the experimental data shows, depicted in Fig. 15, concludes that the model successfully reproduces the impact phenomena.

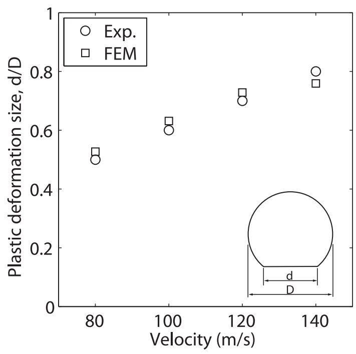

Fig. 15 The size of the plastic deformation on the projectile at various impact velocities.

3.2. The Ceramic Damage Models

The second crucial aspect involved in the present numerical study is selection of the material damage model. A number of models that suitable for the brittle materials has been proposed[(2), (5), (12)–(21)], and following, we evaluate three prominent material models for modeling ceramic damages. They are the modified Tuler-Butcher brittle damage model, the Johnson-Holmquist material model, and the brittle damage model.

The first material model evaluated in this work is the modified Tuler-Butcher brittle damage model[(15), (22)], and is one that provided a reasonable good result with respect to the present experimental data. In this material model, the damage occurs when the maximum principal stress, σ_1, is greater than the material intact strength, σ_0:

$$\int_0^t [\max(0, \sigma_1 - \sigma_0)]^2 \, dt \geq K_f. \tag{1}$$

As shown in Eq. (1), the damage is initiated not only when the stress is higher than the intact strength but also when the measure of the total accumulated damage, K_f, is exceeded. For the present work, those data are obtained from the elastic impact analysis where the impact speed is set to 120 m/s. At this velocity, the experiment has shown the ceramic was intact during the test.

The Johnson-Holmquist (JH) material model has been widely used in studying the response and damage evolution of ceramic materials at an extremely high strain rate. Those studies showed that the model accurately predicts the mechanical responses of a number of ceramic materials. Reference (18), for an example, utilized the model to study impact of a long rod against a silicon carbide, and showed that the prediction is in a good agreement with the experimental data. In addition, References (17) and (19) showed that the JH material model satisfactorily estimated the elastic responses of the boron-carbide and silicon-carbide plates. And finally, Reference (5) demonstrated that the model successfully simulated fragmentation of an alumina ceramic sandwiched with a rubber and a glass/epoxy composite. Because the material model has been widely adopted, currently the model can be found in many finite element and finite volumes codes such as AUTODYN[18], LS-DYNA[2], CTH and EPIC.

The Johnson-Holmquist material assumes that the material strength, von Misses equivalent stress, can be written as a power-law function of hydrostatic pressure[(13),(16),(17),(19)]:

$$\sigma_i^* = A(P^* + T^*)^N (1 + C \ln \dot{\varepsilon}^*) \quad \text{for } D = 1, \quad \text{and} \tag{2}$$

$$\sigma_f^* = B(P^*)^M (1 + C \ln \dot{\varepsilon}^*) \quad \text{for } D = 0, \tag{3}$$

where A, B, C, M, and N are material constants, and D is a scalar damage parameter defined over the range $0 \leq D \leq 1$. The variables σ_i^* and σ_f^* are the normalized intact and fracture strengths of material, respectively. Those stresses are dimensionless by normalizing them to the equivalent stress at the Hugoniot elastic limit (HEL):

$$\sigma^* = \frac{\sigma}{\sigma_{HEL}}. \tag{4}$$

The pressure, P^*, and the maximum hydrostatic tension, T^*, are normalized to the pressure at HEL, P_{HEL}:

$$P^* = \frac{P}{P_{HEL}}. \tag{5}$$

Although this particular material has shown a good performance for a single-hypervelocity impact case, but it did not accurately predict occurrence of damages in the repeated-impact case. In the repeated impact case, the initiated damage by this particular material model was surrounded by a compressive stress state due to the plastic deformation that occurred upon the application of the previous impact; therefore, the subsequent impact did not able to propagate the damage further.

The last material model was proposed by Govindjee et. al.[14], which is an isotropic elastic-plastic material and has been implemented in LS-DYNA as *MAT_ORIENTED_CRACK. This material model assumes that the yielding occurs at

$$\phi = J_2 - \frac{\sigma_y^2}{3},$$

where J_2 is the second stress invariant, and σ_y is the yield strength, which is a function of the effective plastic strain, ε_{eff}^p, and the plastic hardening modulus, E_p:

$$\sigma_y = \sigma_0 + E_p \varepsilon_{eff}^p.$$

The oriented crack fracture model is based on a maximum principal stress criterion such that the element fails when the maximum principal stress exceeds the input fracture stress, σ_f, and the element fails on a plane perpendicular to the direction of the maximum principal stress(21). However, this particular material model currently is available for the solid element only.

3.3. Simulation Results

Two most relevant simulation results of the present work are presented and discussed in this section. They are the history of the first principal stress, Fig. 16, and the damage evolution due the repeated impact, Fig. 17, at the impact velocity of 140 m/s.

The history, Fig. 16, suggests that the highest first principal stress occurred at 0.285 μs, which is significantly shorter than the contact duration of 6.4 μs. During the time, the ceramic was mainly in the compressive stress state, but a small concentric area in the surface of the ceramic was in tension. Until the time of 0.120 μs, the figure clearly shown that the front of the stress wave propagates concentrically. The points where the maximum stress occurred gradually shift away from the axis. After this time, the location of the maximum first principal stress is difficult to be predicted.

The complex stress state after 0.120 μs is likely due to the complex interaction between the sphere and the ceramic, as shown in Fig. 14, rather than the reflected waves within the ceramic. The reflected stress wave in the ceramic itself requires longer time to return to the specimen impacted surface; for instance, the longitudinal waves require about 1.0 μs to reach the specimen impacted surface. The numerical analysis seems to indicate that the high stress state at 0.285 μs is mainly governed by the interaction of the sphere and the ceramic.

Figure 17 shows that initially the cracks propagated in parallel, and then the stress state on the subsequent impact altered the direction of one of the crack, which finally led to the spall fracture. In the present model, when the specimen was impacted eight times, the cone crack has reached a length of 200 μm; meanwhile, in the experiment, 500 impacts were required. However, when the cone crack reached this length, further impacts did not extend the crack any longer in both experiment and simulation. In the simulation, the length of the element size and the total accumulative damages parameter, K_f, fully control the size of the crack extension. Therefore, those parameters should be refined, at a cost of increasing the computation time, to fully reproduce the experimental results

4. Summary and Conclusions

This research on characteristics of a silicon nitride plate has provided an insight of the damage formation on the plate due to the repeated impact against a small but hard particle. Current finding suggests that the ring cracks occurred within a very short time after the projectile touched the ceramic, significantly shorter than the time to the reach maximum contact area. Further application of impacts grew the cracks, which finally led to spalls or a cone crack. However, it is still extremely difficult to accurately quantify the growth of the cracks and their relation to the impactor frequency and velocity.

References

(1) C. Kaufmann, D. S. Cronin, M. J. Worswick, G. Pageau, and A. Beth. Influence of material properties on the ballistic performance of ceramics for personal body armor. *Shock and Vibration Journal*, SAV 10(1):51–59, 2003.

(2) Duane S. Cronin, Khahn Bui, Christian Kaufmann, Grant McIntost, and Todd Berstad. Implementation and validation of the johnson-holmquist ceramic material model in ls-dyna. In *4-th European LS-DYNA Users Conference*, pages DI–47–DI–60, 2003.

(3) J. Zhai and M. Zhou. Finite element analysis of micromechanical failure modes in a heterogeneous ceramic material system. *International Journal of fracture*, 101:161–180, 2000.

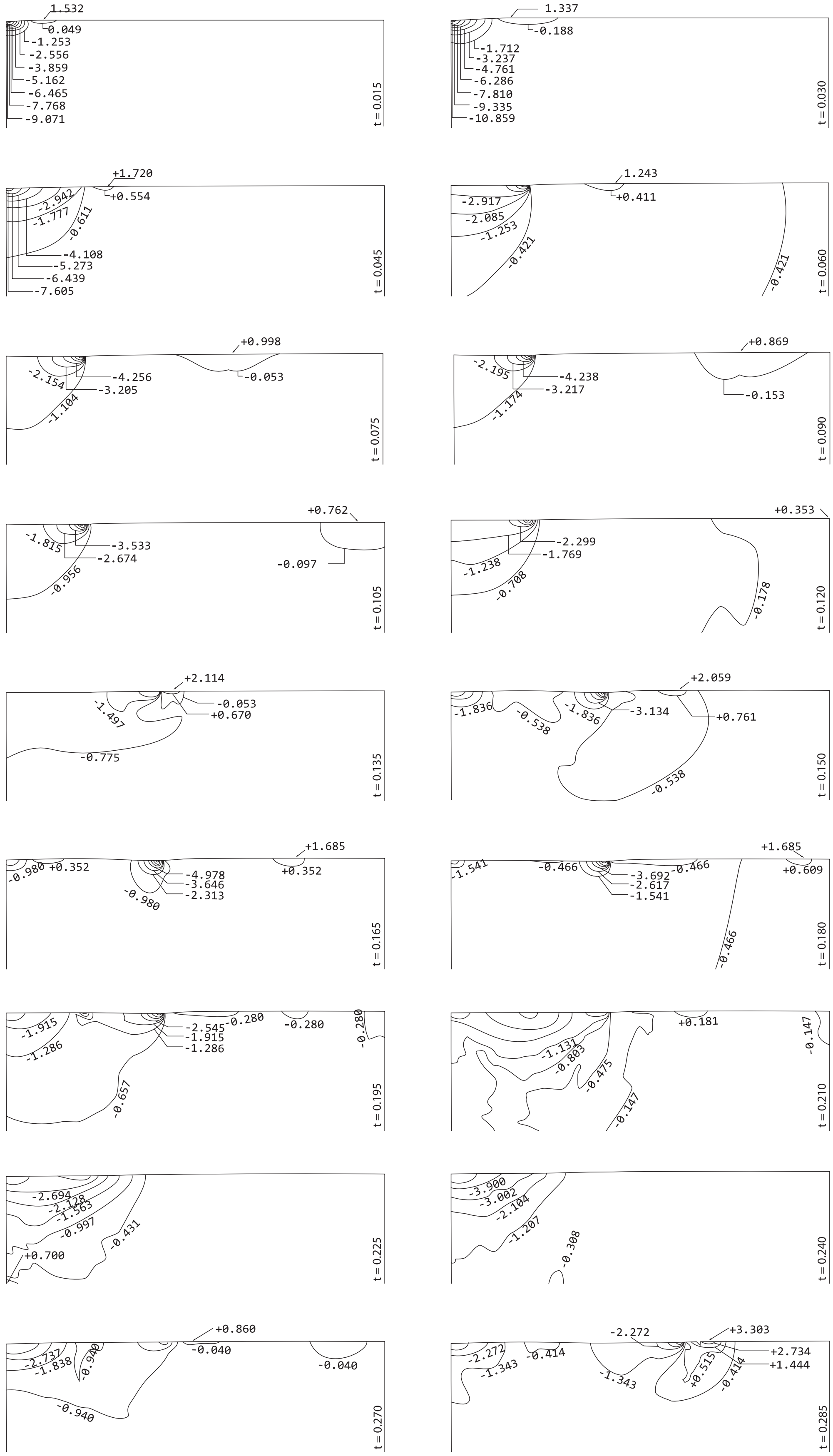

Fig. 16 The distribution of the first principal stress on the damaged area, an area within a radius of 0.5 mm, during impact until the first element failed at 0.285 μs.

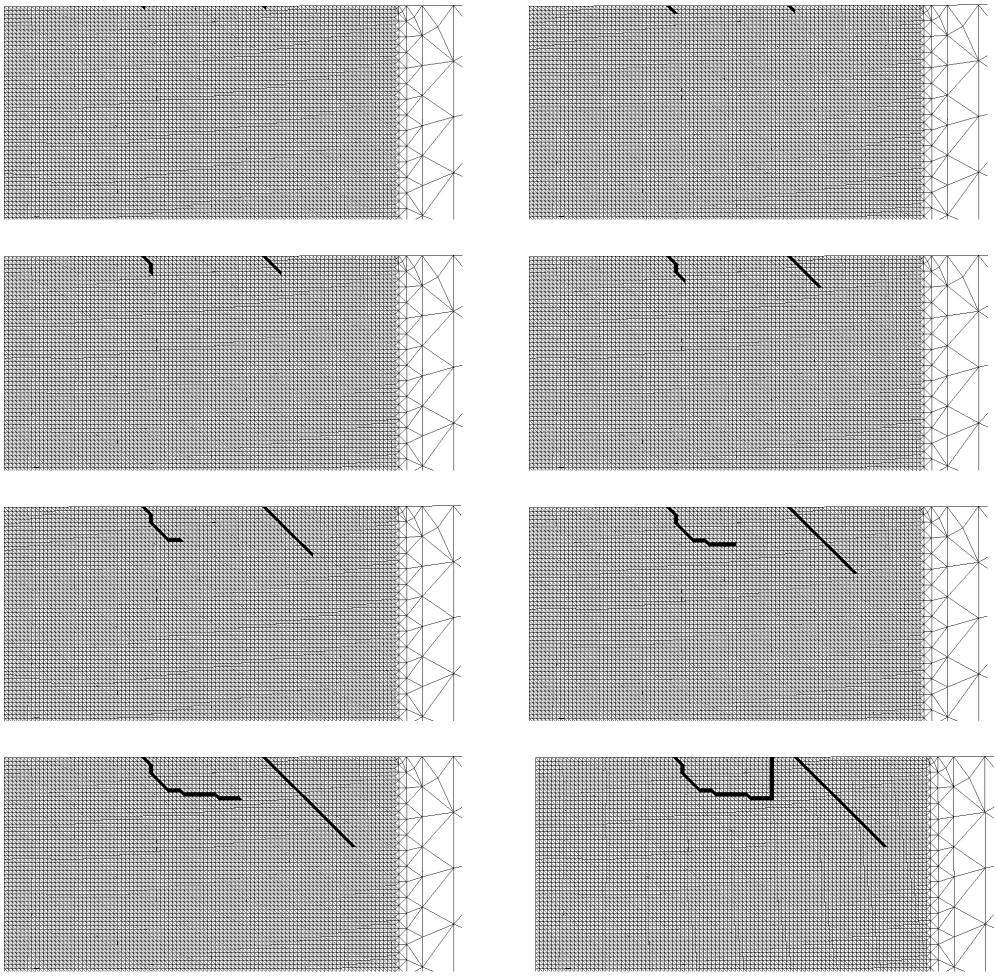

Fig. 17 Formation of damages due to the repeated impacts. The impact frequency is subsequently increases from one to eight. The top-left figure is after one impact, and the bottom-right figure is after eight impact.

(4) T. J. Vogler, W. D. Reinhart, and L. C. Chhabildas. Dynamic behavior of boron carbide. *Journal of applied physics*, 95(8):4173–4183, 2004.

(5) A. Tasdemirci and I. W. Hall. Numerical and experimental studies of damage generation in multi-layer composite materials at high strain rates. *International Journal of Impact Engineering*, 34:189–204, 2007.

(6) P. Lundberg, R. Renstrom, and B. Lundberg. Impact of metallic projectiles on ceramic targets: transition between interface defeat and penetration. *International Journal Impact Engineering*, 24:259–275, 2000.

(7) Raymond L. Woodward. A simple one-dimensional approach to modelling ceramic composite armour defeat. *Internation journal of impact engineering*, 9(4):455–474, 1990.

(8) R. Delagrave. A numerical investigation of the results scatter obtained with the depth of penetration technique. Technical Report DREV-TM-9612, Defence R & D Canada, 1997.

(9) Christian Kaufmann, Duane Cronin, Michael Worswick, Gilles Pageau, and Andre Beth. Influence of material properties on the ballistic performance of ceramics for personal body armour. *Shock and Vibration*, 10:51–58, 2003.

(10) Pruettha Nanakorn. Finite element analysis of crack localization: the smeared crack approach with a mixed formulation. *Thammasat international journal of science and technology*, 5(3):28–39, 2000.

(11) A. V Potapov, M. A. Hopkins, and C. S. Campbell. A two-dimensional dynamic simulation of solid fracture part 1: Description of the model. *International Journal of Modern Physics C*, 6:371–398, 1995.
(12) Andrei A. Gusev. Finite element mapping for spring network representations of the mechanics of solids. *Phys. Rev. Lett.*, 93(3):034302, Jul 2004.
(13) G. R. Johnson and T. J. Holmquist. An improved computational constitutive model for brittle materials. *High pressure science and technology (1993), Edited by S. C. Schmidt, J. W. Shaner, G. A. Samara, and M. Ross*, 2:981–984, 1994.
(14) S. Govindjee, J. G. Kay, and J. C. Simo. Anisotropic modeling and numerical simulation of brittle damage in concrete. *International journal numerical method in engineering*, 38:3611–3633, 1995.
(15) D. R. Faux. Brittle damage models in dyna2d. Technical report, Lawrence Livermore National Laboratory, September 1 1997.
(16) George A. Gazonas. Implementation of the johnson-holmquist ii (jh-2) constitutive model into dyna3d. Technical Report ARL-TR-2699, US Army Research Laboratory, March 2002.
(17) Timothy J. Holmquist and Gordon R. Johnson. Charaterization and evaluation of silicon carbide for high-velocity impact. *Journal of applied physics*, 97:093502.1–093502.12, 2005.
(18) X. Quan, R. A. Clegg, M. S. Cowler, N. K. Birnbaum, and C. J. Hayhurst. Numerical simulation of long rods impacting silicon carbide targets using jh-1 model. *International Journal of Impact Engineering*, 33:634–644, 2006.
(19) T. J. Holmquist and G. R. Johnson. Characterization and evaluation of boron carbide for plate-impact conditions. *Journal of applied physics*, 100:093525–1–093525–13, 2006.
(20) *LS-DYNA Theory Manual*, May 1999.
(21) *LS-DYNA Keywords User's Manual*, May 1999.
(22) F. R. Tuler and B. M. Bucther. A criterion for the time dependence of dynamic fracture. *International Journal of Fracture Mechanics*, 4:4, December 1968.